particles

IMPACT FACTOR 2.3

CITESCORE 3.0

Review

Multimessenger Studies with the Pierre Auger Observatory

Jon Paul Lundquist and the Pierre Auger Collaboration

Special Issue

Selected Papers from the 13th International Conference on New Frontiers in Physics (ICNFP 2024)

Edited by

Prof. Dr. Larissa Bravina, Prof. Dr. Sonia Kabana and Prof. Dr. Armen Sedrakian

MDPI

https://doi.org/10.3390/particles8020045

particles

MDPI

Review

Multimessenger Studies with the Pierre Auger Observatory †

Jon Paul Lundquist [1,*] and the Pierre Auger Collaboration [2,‡]

[1] Center for Astrophysics and Cosmology (CAC), University of Nova Gorica, 5000 Nova Gorica, Slovenia
[2] Observatorio Pierre Auger, Av. San Martín Norte 304, Malargüe 5613, Argentina; spokespersons@auger.org
* Correspondence: jlundquist@ung.si
† This paper is based on the talk at the 13th International Conference on New Frontiers in Physics (ICNFP 2024), Crete, Greece, 26 August–4 September 2024.
‡ Full author list is in Acknowledgments.

Abstract: The Pierre Auger Observatory, the world's largest ultra-high-energy (UHE) cosmic ray (CR) detector, plays a crucial role in multi-messenger astroparticle physics with its high sensitivity to UHE photons and neutrinos. Recent Auger Observatory studies have set stringent limits on the diffuse and point-like fluxes of these particles, enhancing constraints on dark-matter models and UHECR sources. Although no temporal coincidences of neutrinos or photons with LIGO/Virgo gravitational wave events have been observed, competitive limits on the energy radiated in these particles have been established, particularly from the GW170817 binary neutron star merger. Additionally, correlations between the arrival directions of UHECRs and high-energy neutrinos have been explored using data from the IceCube Neutrino Observatory, ANTARES, and the Auger Observatory, providing additional neutrino flux constraints. Efforts to correlate UHE neutron fluxes with gamma-ray sources within our galaxy continue, although no significant excesses have been found. These collaborative and multi-faceted efforts underscore the pivotal role of the Auger Observatory in advancing multi-messenger astrophysics and probing the most extreme environments of the Universe.

Keywords: high-energy particle physics; astrophysics; ultra-high energy cosmic rays; neutrinos; gravitional waves

Academic Editors: Larissa Bravina, Sonia Kabana and Armen Sedrakian

Received: 7 February 2025
Revised: 28 February 2025
Accepted: 19 April 2025
Published: 22 April 2025

Citation: Lundquist, J.P.; the Pierre Auger Collaboration. Multimessenger Studies with the Pierre Auger Observatory. *Particles* **2025**, *8*, 45. https://doi.org/10.3390/particles8020045

1. Introduction

The Pierre Auger Observatory (Auger), the world's largest detector of ultra-high-energy cosmic rays (UHECRs; nuclei with $E > 10^{18}$ eV), is a key instrument in multimessenger astroparticle physics [1]. Its hybrid configuration of a large-scale ∼1600 component surface detector (SD) and four air fluorescence detector sites also enables high-sensitivity searches for UHE photons and neutrinos, which provide important clues about the nature of UHECR sources and potential exotic phenomena. Auger's limits on diffuse and point-like fluxes ($cm^{-2}\ s^{-1}\ GeV^{-1}$) of these neutral messengers constrain dark-matter models, Lorentz invariance violation scenarios, and the physics of most energetic cosmic accelerators.

No neutrino or photon candidates have yet been found in coincidence with gravitational wave events detected by LIGO/Virgo. However, competitive upper limits on the associated energy emission have been established, including constraints from the binary neutron star merger GW170817. Joint analyses with the IceCube Neutrino Observatory and ANTARES have revealed no significant directional correlations between UHECRs and high-energy neutrinos, refining neutrino flux limits. Additionally, searches for UHE neutrons originating from Galactic gamma-ray sources have not yet yielded evidence of point-like

excesses, but have provided stringent limits on their flux. Each of these non-detections refines theoretical models and narrows the parameter space for astrophysical scenarios.

In the following, we review recent neutrino searches, potential neutrino emissions from gravitational wave events, correlation analyses between UHECRs and high-energy neutrinos, and searches for neutron signals from gamma-ray sources. We then discuss the future outlook for multimessenger observations with the Pierre Auger Observatory.

2. Neutrino Search

Neutrinos (ν) are produced by UHECRs through interactions during propagation (cosmogenic ν) and at UHECR sources themselves (astrophysical ν). Neutrinos have extremely small cross-sections, allowing them to travel vast cosmic distances with minimal absorption (unlike UHE photons, which more strongly interact with radiation fields). As neutral particles, they are also undeflected by magnetic fields, making them ideal for studying the high-energy universe.

Auger is sensitive to neutrinos with energies $E_\nu > 10^{17}$ eV [2,3]. Neutrino-induced air showers are expected to have a strong electromagnetic (EM) signature at large zenith angles and a weak muonic component. In contrast, hadronic showers have their EM component absorbed high in the atmosphere. The result is distinct SD signals allowing efficient neutrino discrimination, including the high EM component, an extended time spread, and a high average signal area relative to the peak. Three detection channels are defined by the zenith angle: Earth-skimming (90°–95°), and downward-going high (DGH; 75°–90°) and low (DGL; 60°–75°) angles. Sensitivity to Earth-skimming ν_τ events is particularly large due to the Earth's crust's large target mass.

An intensive search using data from 2004 to 2021 has identified no neutrino candidates. As a result, stringent upper limits on diffuse and point-like neutrino fluxes (Figure 1) have been established, placing strong constraints on cosmogenic neutrino models. In particular, scenarios involving pure-proton UHECR composition with strong source evolution are excluded [4]. Figure 1 shows that the Auger differential limits are competitive with those from IceCube and ANITA at overlapping energies and provide the strongest limits between 10^{18} to 10^{19} eV. Auger's results also contribute significantly to multimessenger studies, providing constraints on neutrino emission associated with gravitational wave events and other astrophysical transients, as will be discussed in the following sections.

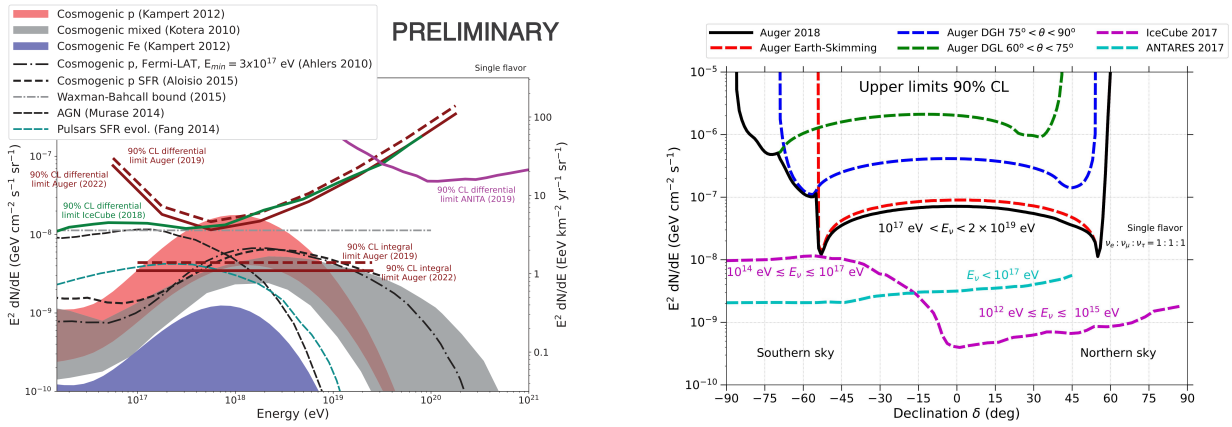

(**a**) (**b**)

Figure 1. (**a**) Diffuse neutrino flux upper limits (integral: straight lines, differential: curved lines) compared with expectations from [3]. (**b**) and declination dependent "point-source" flux upper limits from [5].

3. Neutrinos and Gravitational Waves

3.1. Binary Black Hole Merger Neutrinos

Auger's sensitivity to UHE neutrinos enables follow-up studies of gravitational wave (GW) events, such as binary black hole (BBH) mergers. The following stacking analysis examines all BBH mergers observed by LIGO and Virgo during the observation runs O1 to O3 [2]. It expands upon the analysis in [6] and utilizes the neutrino sensitivity methods described in [5]. The analysis assumes isotropic UHE neutrino emission with an E_ν^{-2} spectrum and calculates the 90% confidence interval (CI) upper limits on the luminosity $L_{\mathrm{up},i}$ as

$$L_{up,i} = \frac{N_{up,\nu}}{T_i} \left(\sum_s \sum_{p \in \Omega_{90}(s)} A_{p,s,i} P_{p,s} \int_0^\infty \frac{\Pi_{p,s}(r)}{r^2 (1+z(r))}\, dr \right)^{-1} \tag{1}$$

where the parameter definitions are given in Table 1.

Table 1. Definitions of parameters used in the neutrino upper-limit luminosity calculation of Equation (1).

Parameter Definitions for Equation (1)	
Indices s: BBH Merger, p: Healpix Pixel Locations	$N_{\mathrm{up},\nu} = 2.44$: ν Non-observation 90% CL (Section 2)
T_i : Neutrino Emission Time Window	$p \in \Omega_{90}(s)$: Pixels inside 90% CL Solid Angle of Source s
$P_{p,s}$: GW Source Probability (PDF) at Pointing Direction	$\Pi_{p,s}(r)$: GW Luminosity Distance PDF
z: Redshift	$A_{p,s,i}$: E_ν^{-2} Integrated Effective Detector Area. Function of Zenith Angle and Time.

The resulting upper-limit neutrino luminosity over a 24 h emission window is $L_{\mathrm{up,1day}} = 2.7 \times 10^{48}$ erg s^{-1}, corresponding to a total neutrino energy of $E_{\mathrm{up,1day}} = 2.3 \times 10^{53}$ erg. Over a 60 day window, these limits become $L_{\mathrm{up,60days}} = 4.6 \times 10^{46}$ erg s^{-1} and $E_{\mathrm{up,60days}} = 2.4 \times 10^{53}$ erg, $\sim$1/60 of the one-day limits. This corresponds to an upper-limit neutrino output of $\sim$1/20 of the estimated total energy release from BBH mergers ($\sim 2M_\odot c^2$).

Figure 2 presents how the 24 h emission results were attained from the combined analysis of 83 BBH mergers across three LIGO/Virgo observation runs (O1–O3). These constraints provide valuable insights into UHE neutrino emissions from GW events, aiding multimessenger studies.

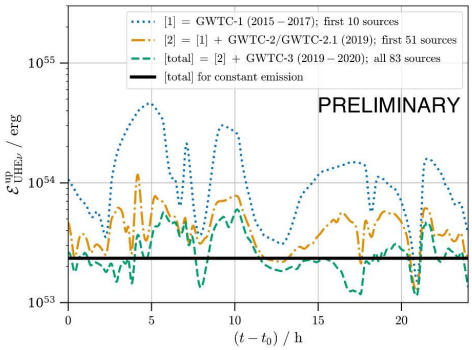

Figure 2. Stacking analysis upper limits on UHE ν emission over a 24 h time window for BBH mergers from [2]. Solid line: $E_{\mathrm{up,1day}} = 2.3 \times 10^{53}$ erg the upper limit on the total energy emitted in the UHE neutrinos. Dashed lines: partial results for each source subset.

3.2. Binary Neutron Star Merger Neutrinos

Auger performed a follow-up search for UHE neutrinos associated with the gravitational wave event GW170817, a binary neutron star (BNS) merger detected by LIGO and Virgo [7]. This BNS was seen by 70 observatories (7 continents and space) across the EM spectrum. The Auger analysis was c onducted in a $\pm$500 s time window around the merger event and extended up to 14 days post-trigger. During this interval, the event was optimally situated within the Earth-skimming (ES) sensitivity band (zenith angles $90^\circ < \theta < 95^\circ$) as shown in Figure 3a.

The non-observation of UHE neutrinos allowed Auger to set the most stringent upper limits on neutrino spectral fluence for energies 100 PeV $\leq E_\nu \leq$ 25 EeV, complementing IceCube and ANTARES results. Figure 3b shows the upper limits derived for this event, highlighting Auger's sensitivity to UHE neutrinos during multimessenger follow-ups.

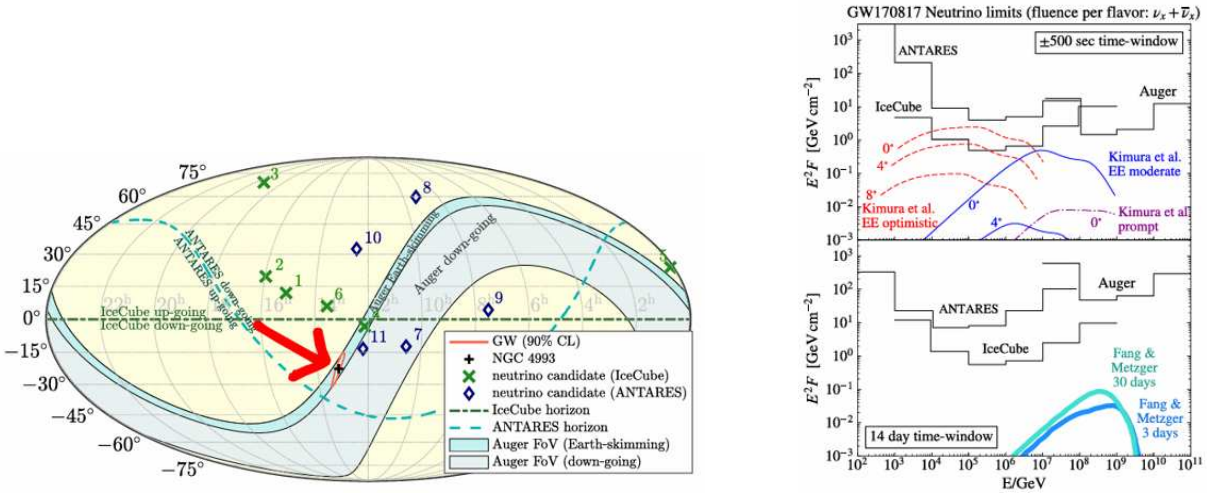

(**a**) (**b**)

Figure 3. (**a**) Sky map of the GW170817 location and the Auger field-of-view. (**b**) The resulting upper limits on the neutrino spectral fluence derived by Auger, IceCube, and ANTARES for the $\pm$500 s time window [7].

4. UHECR and Neutrinos

This section is a short review of the search for spatial correlations of neutrinos with UHECR published in 2022 using data up to 2017 [8,9]. This study was the product of $\sim$1000 authors using neutrino data from ANTARES and IceCube, and UHECR from Auger and Telescope Array collaborations.

4.1. Arrival Direction Cross-Correlation

The arrival directions of UHECRs and neutrinos can be analyzed for correlations to identify potential common origins. This analysis considers the number of observed UHECR–neutrino pairs, $n_{\rm obs}$, within an angular separation δ, and compares it to the expected number $\langle n_{\rm exp} \rangle$ under two null-hypotheses: isotropic UHECRs or neutrinos. The test statistic (TS) used quantifies the relative excess of pairs over the expectation:

$$\mathrm{TS} = \max\left(\frac{n_{\rm obs}(\delta_i)}{\langle n_{\rm exp}(\delta_i) \rangle} - 1 \right) \tag{2}$$

where the separation δ is the free parameter.

The most significant result appears in the case of isotropic neutrinos, where the analysis randomizes neutrino arrival directions while keeping UHECR data fixed. This

procedure scans angles for significant clustering at distances δ from 1° to 30° in 1° steps. Figure 4 shows the relative excess of UHECR–neutrino pairs as a function of angular distance for isotropic neutrinos. The results are compatible with neutrino background expectations, yielding post-trial p-values of 0.23 for track-like neutrino events and 0.15 for cascade-like events.

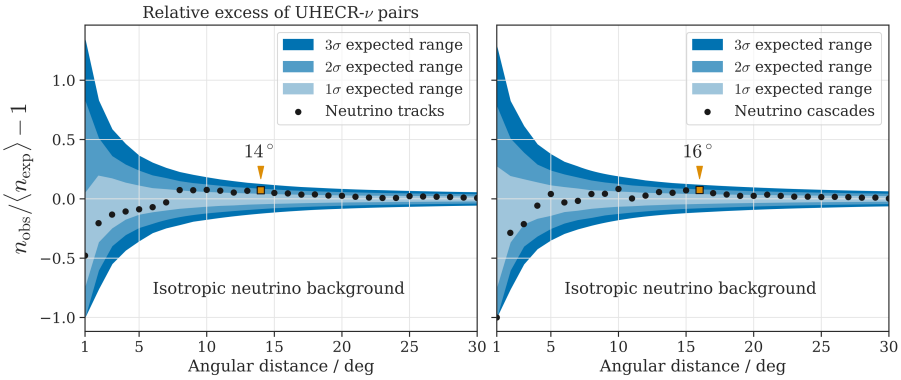

Figure 4. Relative excess of UHECR–neutrino pairs as a function of angular separation δ. The observed data (solid lines) are compared to the isotropic neutrino background. The maximum significance scan angle for the two different neutrino signals are shown by the arrows. Taken from [8].

4.2. UHECR Excess Around High-Energy Neutrinos

This analysis investigates potential correlations between UHECRs and high-energy neutrinos, assuming the latter as possible source locations of UHECRs. The background hypothesis assumes an isotropic UHECR flux, while the signal hypothesis considers clustering around neutrino arrival directions accounting for UHECR magnetic deflection.

The analysis uses an unbinned likelihood stacking method to test the number of UHECR signal events n_s, treated as a free parameter. The likelihood function is defined as

$$\ln \mathcal{L}(n_s) = \sum_{\mathcal{E} \in \{\text{Auger,TA}\}} \sum_{i=1}^{N_\mathcal{E}} \ln\left(\frac{n_s}{N_{\text{CR}}} S_i^\mathcal{E} + \frac{N_{\text{CR}} - n_s}{N_{\text{CR}}} B_i^\mathcal{E} \right) \tag{3a}$$

$$S_i^\mathcal{E}(\delta_i, E_i) = R_\mathcal{E}(\delta_i) \sum_{j=1}^{N_{\text{src},\nu}} S_{ij}\left(\vec{\Omega}_i, \sigma_i(E_i)\right), \tag{3b}$$

$$\sigma_i(E_i) = \sqrt{\sigma_\mathcal{E}^2 + \sigma_{\text{MD}}^2(E_i)} \tag{3c}$$

where the parameter definitions for Equations (3a)–(3c) are summarized in Table 2. Figure 5 shows an example likelihood map for neutrino shower-like events along with UHECR arrival directions. To evaluate the significance of a possible excess, the test statistic is the log-likelihood ratio $-2\ln\left(\frac{\mathcal{L}(\hat{n}_s)}{\mathcal{L}(n_s=0)}\right)$ and has an approximate χ^2 isotropic distribution.

Three magnetic deflections, $\sigma_{\text{MD}} = D \cdot \frac{100\ \text{EeV}}{E}$, were tested due to composition and magnetic field uncertainties. The results are consistent with an isotropic UHECR distribution. The most significant pre-trial p-values were 0.23 for track-like neutrino events and 0.15 for cascade-like events with UHECR deflection ∼10°. The findings also highlight significant uncertainties due to composition and intergalactic magnetic fields, which impact clustering.

Table 2. Definitions of parameters for calculating UHECR clustering likelihood around the HE neutrino sources of Equations (3a)–(3c).

Parameter Definitions for Equations (3a)–(3c)	
n_s: # of Signal UHECR (Free Parameter)	$N_{CR} = N_{TA} + N_{Auger}$: Total UHECR Number
$S^i_{\mathcal{E}}$: UHECR Event i Signal Probability	$B^i_{\mathcal{E}}$: UHECR i Background Probability (Exposure)
δ_i : Declination of UHECR Event i	$R_{\mathcal{E}}(\delta_i)$: Relative Exposure at δ_i
S_{ij}: 2-d Gaussian Around ν Source j	$\overrightarrow{\Omega}_i$: UHECR Event Pointing-direction
$\sigma_i(E_i)$: Combined Angular Uncertainty. ν Gaussian STD.	$\sigma_{\mathcal{E}}$: Detector Angular Resolution
$\sigma_{MD}(E_i)$: Magnetic Deflection as a Function of Energy	

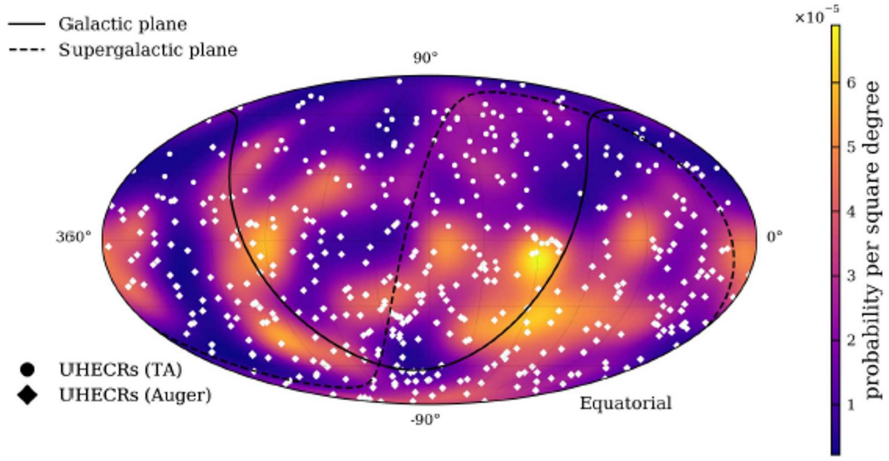

Figure 5. Stacked likelihood map of neutrino shower–like events and UHECR arrival directions [8]. The color scale shows the probability of UHECR clustering around high-energy neutrinos as the source locations.

4.3. Neutrino Excess Around Extreme UHECR

This analysis investigates potential correlations between the highest-energy UHECRs (E > 70 EeV) and neutrinos, assuming UHECR as possible source locations of neutrinos. The background hypothesis is an isotropic neutrino flux, while the signal hypothesis considers clustering around UHECR arrival directions accounting for magnetic deflection.

To test this hypothesis, a likelihood-based approach is used like the previous section. The log-likelihood function incorporates the observed neutrino and UHECR events, their spatial distribution, and angular uncertainties and is defined as

$$\ln \mathcal{L}(n_s, \gamma_s) = \underbrace{\sum_{j=1}^{N_{CR}}}_{\text{Stacking, step 3}} \Bigg[\underbrace{\sum_{i=1}^{N_\nu} \ln\left(\frac{n_s}{N_\nu} S^i_\nu(\gamma_s, \overrightarrow{\Omega}_s) + \frac{N_\nu - n_s}{N_\nu} B^i_\nu(\overrightarrow{\Omega}_s) \right)}_{\text{Neutrino data, step 1}} - \underbrace{\frac{(\overrightarrow{\Omega}_s - \overrightarrow{\Omega}_j)^2}{\sigma_j(E_j)^2}}_{\text{UHECR data, step 2}} \Bigg]. \quad (4)$$

where the parameters used are summarized in Table 3. Step one is the neutrino source likelihood test statistic $\ln\left(\frac{\mathcal{L}(\hat{n}_s, \hat{\gamma}_s)}{\mathcal{L}(n_s=0)}\right)$ and is shown in Figure 6 (left). Step two is the log of the UHECR gaussian shown in Figure 6 (center). Step three sums over all UHECR.

Three magnetic deflection scenarios were tested using the same scaling as the previous section. The most significant pre-trial p-value of $p = 0.097$ was found for a deflection angle of $D = 6^\circ$ and an energy threshold of $E_{cut} = 85$ EeV. While this suggests a modest excess, it remains consistent with an isotropic neutrino distribution after accounting for scan penalties.

UHECR composition and magnetic field uncertainties significantly affect the analysis sensitivity, as these determine the magnitude of the magnetic deflection. Constraining these uncertainties further is required to improve sensitivity to UHECR–neutrino correlations.

Table 3. Definitions of parameters used in the analysis of Equation (4).

Parameter Definitions for Equation (4)	
n_s: Number of Signal Events (Free Parameter)	γ_s: ν Source Spectrum Index (Free Parameter)
N_{CR}, N_ν: UHECR and Neutrino Event Counts	S_ν^i: ν Event i Signal Probability
B_ν^i: Event i Background Probability	$\overrightarrow{\Omega}_s$: Healpix Grid Point Pointing-direction
$\overrightarrow{\Omega}_j$: UHECR Pointing-direction	$\sigma_j(E_j)$: Combined Angular Uncertainty

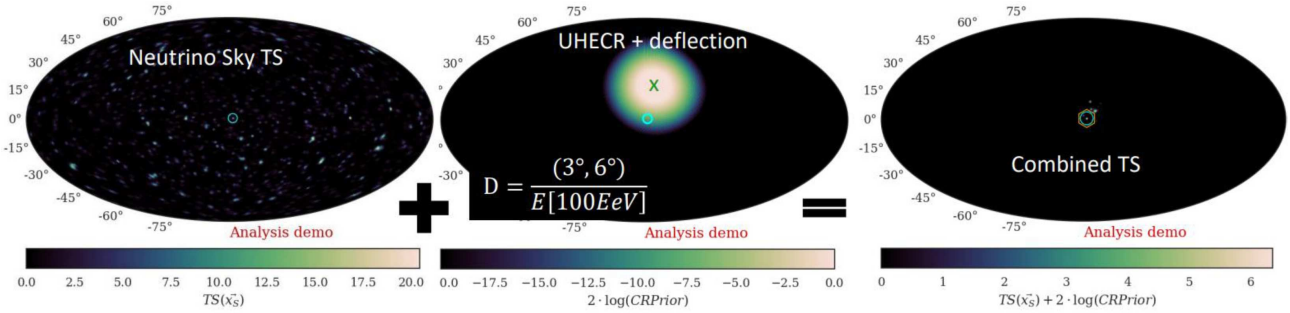

Figure 6. Stacked likelihood maps example for one UHECR event taken from the presentation of [9], demonstrating the steps of Equation (4).

5. Neutrons and Galactic Gamma-Rays

Neutrons provide another unique opportunity to identify UHECR sources as they also travel undeflected by interstellar magnetic fields. Neutrons are primarily generated through photodisintegration or pion production processes from UHECR interactions with interstellar photon fields. Gamma-ray sources are natural candidates for neutron production as they indicate regions of high-energy particle acceleration where these processes occur. Although neutrons are unstable, with a rest-frame mean lifetime of 15 min, ultra-high-energy neutrons can travel significant distances before decaying. Their mean travel distance is given by $\langle D \rangle = 9.2\,\mathrm{kpc} \times \frac{E_N}{\mathrm{EeV}}$, allowing for potential detection within galactic scales.

This section reviews the 2023 analysis from [10], which updates [11]. As neutron-induced extensive air showers are indistinguishable from those caused by protons, a neutron flux is inferred from an excess density of UHECRs arriving from specific gamma-ray source directions. This density is estimated using the weighted sum of events

$$\rho_j^{\mathrm{obs}} = \sum_{i=1}^{N} w_{ij} = \sum_{i=1}^{N} \frac{1}{2\pi\sigma_i^2} \exp\left(-\frac{\xi_{ij}^2}{2\sigma_i^2}\right), \tag{5}$$

where ξ_{ij} is the angular distance between UHECR i and target j, and σ_i is the angular uncertainty, parameterized as a function of zenith angle θ and number of triggered SD.

The analysis uses an updated 18 years of Auger data, significantly increasing the exposure and field of view, enabling neutron searches from sources such as the Crab Nebula for the first time. Observed excess significance is determined by counting isotropic simulations with a larger ρ_j. To account for multiple testing across a source class set, the penalized p-value for the most significant source target is $p^* = 1 - (1 - p)^N$. The result is that no significant neutron flux has been observed in any gamma-ray source class.

For $E_{CR} \geq 1$ EeV Table 4 summarizes the most significant target in each source class, penalized target p-values, source class flux ULs, and source class p-values (including the

total weighted by detector exposure at each source location, electromagnetic flux, and expected neutron decay flux attenuation). Table 5 shows only the entries with the smallest p-values for $E_{CR} \geq 0.1$ EeV. The most significant result is obtained for H.E.S.S. pulsar wind nebula with $E_{CR} \geq 1$ EeV, yielding a weighted p-value of 0.0052. The most significant source target was a gamma-ray pulsar with a p^*-value 0.013 again for $E_{CR} \geq 1$ EeV.

Table 4. Most significant target from each target set $E_{CR} \geq 1$ EeV (assuming an E^{-2} spectrum).

	Most Significant Source				Total Source Class			
Class	**R.A.**	**Dec.**	***p*-Val**	***p****	**Flux U.L.**	**E-Flux U.L.**	***p*-Val**	***p*-Val (Weighted)**
msec PSRs	286.2	2.1	0.0075	0.88	0.026	0.19	0.90	0.50
γ-ray PSRs	296.6	−54.1	5.0×10^{-5}	0.013	0.023	0.17	0.16	0.020
LMXB	237.0	−62.6	0.0069	0.51	0.017	0.12	0.62	0.25
HMXB	308.1	41.0	0.014	0.57	0.13	0.97	0.49	0.34
H.E.S.S. PWN	128.8	−45.6	0.0070	0.18	0.016	0.12	0.24	0.0052
H.E.S.S. other	128.8	−45.2	0.022	0.63	0.014	0.11	0.52	0.22
H.E.S.S. UNID	305.0	40.8	0.0066	0.31	0.15	1.1	0.61	0.75
Microquasars	308.1	41.0	0.014	0.19	0.13	0.95	0.39	0.81
Magnetars	249.0	−47.6	0.15	0.99	0.011	0.079	0.99	0.98
LHAASO	292.3	17.8	0.024	0.20	0.038	0.28	0.22	0.42
Crab	83.6	22.0	0.71	...	0.22	0.15	0.71	...
Gal. Center	266.4	−29.0	0.86	...	0.0053	0.039	0.86	...

Table 5. Most significant results for $E_{CR} \geq 0.1$ EeV (assuming an E^{-2} spectrum).

	Most Significant Source				Total Source Class			
Class	**R.A.**	**Dec.**	***p*-Val**	***p****	**Flux U.L.**	**E-Flux U.L.**	***p*-Val**	***p*-Val (Weighted)**
H.E.S.S. other	288.2	10.2	0.0033	0.036	5.5	40.2	0.074	0.58
Magnetars	274.7	−16.0	0.13	0.44	1.6	11.8	0.31	0.14

6. Outlook

In this work, we presented an overview of recent multimessenger analyses with the Pierre Auger Observatory, incorporating UHECRs, neutrinos, gravitational waves, gamma rays, and galactic neutrons. Although no detections were made, these analyses set some of the most stringent upper limits in ultra-high-energy multimessenger astronomy, demonstrating Auger's important role in constraining theoretical models.

The upcoming AugerPrime upgrade [12], nearing completion, will significantly enhance the detector sensitivity and event reconstruction capabilities. By deploying scintillation detectors on top of the surface stations, AugerPrime will improve the separation of electromagnetic and muonic shower components, refining the identification of cosmic-ray primary identification and enhancing energy resolution. Additionally, the installation of radio antennas will enable the detection of air-shower radio signals, offering an independent method of measuring UHECR properties. These additions will allow for more precise searches for UHE photons and neutrinos, which are key messengers of extreme astrophysical environments, such as binary mergers, active galactic nuclei (AGN), gamma-ray bursts (GRBs), and fast radio bursts (FRBs).

The expected outcome is either a reduction in UHE neutral particle upper limits by ∼0.5 orders of magnitude or the first unambiguous detection of these elusive particles. This in turn increases the likelihood of identifying correlations between them and with known astrophysical sources. Such a breakthrough would provide direct insight into the most energetic cosmic accelerators and begin a new chapter in multimessenger astrophysics.

Funding: Financial support was received from the Slovenian Research Agency (ARIS) Research and Infrastructure Programs (project no. I0-0033 and P1-0031).

Data Availability Statement: No new data were created or analyzed in this study. Data sharing is not applicable to this article.

Acknowledgments: Full author list: https://www.auger.org/archive/authors_2024_09.html, accessed on 18 April 2025.

Conflicts of Interest: The authors declare no conflicts of interest. The funders had no role in the design of the study; in the collection, analyses, or interpretation of data; in the writing of the manuscript; or in the decision to publish the results.

References

1. Aab, A.; Aminaei, A.; Buitink, S.; Coppens, J.M.S.; de Jong, S.J.; De Mauro, G.; Dolron, P.; Falcke, H.; Grebe, S.; Grillo, A.F.; et al. The Pierre Auger Cosmic Ray Observatory. *Nucl. Instrum. Methods Phys. Res. Sect. A* **2015**, *798*, 172–213. [CrossRef]
2. Abdul Halim, A.; Abreu, P.; Aglietta, M.; Allekotte, I.; Cheminant, K.A.; Almela, A.; Aloisio, R.; Alvarez-Muñiz, J.; Yebra, J.A.; Anastasi, G.A.; et al. Latest results from the searches for ultra-high-energy photons and neutrinos at the Pierre Auger Observatory. In Proceedings of the 38th International Cosmic Ray Conference—PoS(ICRC2023), Nagoya, Japan, 26 July–3 August 2023; Volume 444, p. 1488. [CrossRef]
3. Niechciol, M. Searching for neutral particles at the highest energies at the Pierre Auger Observatory. In Proceedings of the 6th International Symposium on Ultra-High Energy Cosmic Rays (UHECR2022), L'Aquila, Italy, 3–7 October 2022; Volume 283, p. 04003. [CrossRef]
4. Abdul Halim, A.; Abreu, P.; Aglietta, M.; Allekotte, I.; Cheminant, K.A.; Almela, A.; Aloisio, R.; Alvarez-Muñiz, J.; Yebra, J.A.; Anastasi, G.A.; et al. Investigating the UHECR characteristics from cosmogenic neutrino limits with the measurements of the Pierre Auger Observatory. In Proceedings of the 38th International Cosmic Ray Conference—PoS(ICRC2023), Nagoya, Japan, 26 July–3 August 2023; Volume 444, p. 1520. [CrossRef]
5. Aab, A.; Abreu, P.; Aglietta, M.; Albuquerque, I.F.M.; Albury, J.M.; Allekotte, I.; Almela, A.; Castillo, J.A.; Alvarez-Muñiz, J.; Anastasi, G.A.; et al. Limits on point-like sources of ultra-high-energy neutrinos with the Pierre Auger Observatory. *J. Cosmol. Astropart. Phys.* **2019**, *2019*, 004. [CrossRef]
6. Schimp, M.; Abreu, P.; Aglietta, M.; Albury, J.M.; Allekotte, I.; Almela, A.; Alvarez-Muniz, J.; Batista, R.A.; Anastasi, G.A.; Anchordoqui, L.A.; et al. Combined Search for UHE Neutrinos from Binary Black Hole Mergers with the Pierre Auger Observatory. In Proceedings of the 37th International Cosmic Ray Conference—PoS(ICRC2021), Berlin, Germany, 12–23 July 2021; Volume 395, p. 968. [CrossRef]
7. Albert, A.; Andre, M.; Anghinolfi, M.; Ardid, M.; Aubert, J.-J.; Aublin, J.; Avgitas, T.; Baret, B.; Barrios-Marti, J.; Basa, S.; et al. Search for High-energy Neutrinos from Binary Neutron Star Merger GW170817 with ANTARES, IceCube, and the Pierre Auger Observatory. *Astrophys. J. Lett.* **2017**, *850*, L35. [CrossRef]
8. Albert, A.; Alves, S.; André, M.; Anghinolfi, M.; Ardid, S.; Aubert, J.-J.; Aublin, J.; Baret, B.; Basa, S.; Belhorma, B.; et al. Search for Spatial Correlations of Neutrinos with Ultra-high-energy Cosmic Rays. *Astrophys. J.* **2022**, *934*, 164. [CrossRef]
9. Schumacher, L. Search for correlations of high-energy neutrinos and ultrahigh- energy cosmic rays. In Proceedings of the VLVnT-2018 Conference, Dubna, Russia, 1–4 October 2018; Volume 207, p. 02010. [CrossRef]
10. Abdul Halim, A.; Abreu, P.; Aglietta, M.; Allekotte, I.; Cheminant, K.A.; Almela, A.; Aloisio, R.; Alvarez-Muñiz, J.; Yebra, J.A.; Anastasi, G.A.; et al. Search for evidence of neutron fluxes using Pierre Auger Observatory data. In Proceedings of the 38th International Cosmic Ray Conference—PoS(ICRC2023), Nagoya, Japan, 26 July–3 August 2023; Volume 444, p. 246. [CrossRef]

11. Aab, A.; Abreu, P.; Aglietta, M.; Ahlers, M.; Ahn, E.J.; Samarai, I.A.; Albuquerque, I.F.M.; Allekotte, I.; Allen, J.; Allison, P.; et al. A Targeted Search for Point Sources of EeV Neutrons. *Astrophys. J. Lett.* **2014**, *789*, L34. [CrossRef]
12. Castellina, A. AugerPrime: The Pierre Auger Observatory Upgrade. In Proceedings of the 2018 International Symposium on Ultra-High-Energy Cosmic Rays-UHECR-2018, Paris, France, 8–12 October 2018; Volume 210, p. 06002. [CrossRef]